GEOPHYSICS, VOL. 44, NO. 9 (SEPTEMBER 1979); P. 1531–1540, 7 FIGS.

Phase-compensating filtering to reduce distortion caused by in-aircraft reactive integrators

Oliver G. Jensen* and Alex Becker‡

Low-pass filters based on reactive integrators necessarily introduce temporal phase delays into data. The use of such filters in airborne geophysical surveys, therefore, produces equivalent spatial phase delays which displace the high-wavenumber Fourier components of anomalies downstream along the flight line, causing distortion of the anomaly shapes. A linear filter is described which eliminates this distortion by introducing a compensating, frequency-dependent phase advance. The restored data provide anomalies as would be seen from an aircraft moving with zero speed. Exact phase compensation for each stage of reactive low-pass filtering requires an acausal filter whose coefficients are a weighted sum of *zero*th- and first-order modified Hankel functions, the weighting being determined by the integrator's time constant. A very short and useful approximation to the ideal phase-compensating filter is also described and subsequently applied in the restoration of data obtained from an airborne electromagnetic (EM) survey flown near Hawksbury, Ontario. The example clearly demonstrates the usefulness of applying phase compensation to geophysical data obtained in high-resolution airborne surveys.

INTRODUCTION

In continuous airborne geophysical measurements, high-frequency "noise" which can mask the geophysical anomaly being sought is usually filtered from the data before it is recorded. The filtering process is accomplished by passing the analog signal voltage through reactive low-pass filters or integrators. Such filters necessarily introduce phase shifts depending upon the frequency of the signal being passed by the filter. As the aircraft moves, these temporal phase shifts are observed as equivalent spatial phase shifts which can seriously distort the apparent shape of a geophysical anomaly. Our purpose is to show how this type of anomaly distortion can be reduced subsequently through reprocessing of the data using a simple phase-compensating filter. The technique will be applied to artificial model anomaly data and also to some actual airborne Tridem® [three-frequency aeroelectromagnetic (AEM) system] survey data obtained over a region near Hawksbury, Ontario.

Phase-compensating filtering should be applicable to virtually all airborne geophysical survey data. Distortion of AEM and aeromagnetic (AMAG) anomalies caused by in-aircraft reactive filtering is a generally well-known phenomenon (Palacky, 1976; Ghosh, 1972). Giret (1962) showed that the time constant of the integration can create a marked effect on the form of aeroradiometric anomalies as well. However, rather than obtaining the phase-compensating deconvolution filter which would have corrected the anomaly distortions, Giret showed that distortion created by integrators was not an *overly serious* problem if the product of the integration time constant and aircraft velocity were sufficiently less than the flight altitude. Using contemporary geophysical equipment along with the appropriate data reprocessing techniques, even this constraint can be somewhat relaxed, resulting in reduced survey time along with an improvement in survey resolution and accuracy. In principle, an airborne survey could be

®Registered trademark of Scintrex Ltd.

Manuscript received by the Editor June 5, 1978; revised manuscript received March 5, 1979.
*Dept. of Mining and Metallurgical Engineering, McGill Univ., 3480 University St., Montreal, Canada H3A 2A7.
‡The Mineral Exploration Research Institute, C. P. 6079, Station A, Montreal, Canada H3C 3A7.

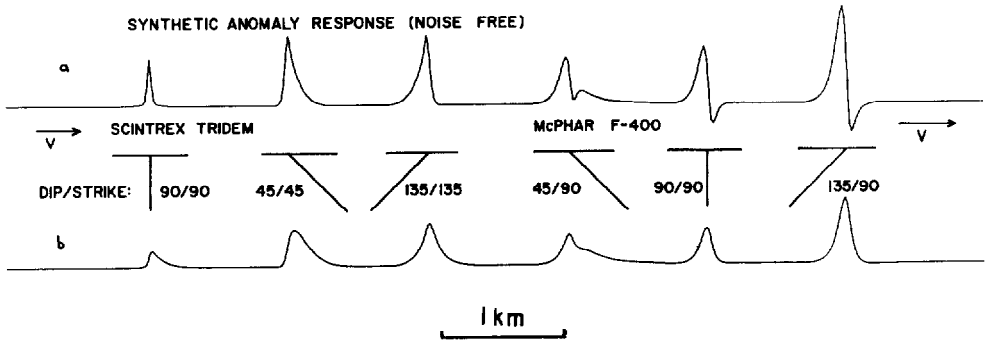

FIG. 1. The distortion of geophysical in-phase AEM anomalies caused by in-aircraft low-pass filtering by reactive integrators. (a) Six synthetic anomalies calculated for the geophysical models shown and for two different AEM transmitter-receiver configurations: The first group of three anomalies shows the response of the Scintrex Tridem system flown at an elevation of 40 m, the second group of three anomalies shows the response of the McPhar F-400 system flown at an elevation of 140 m. (b) The anomalies in (a) after low-pass filtering with an integrator time constant τ of 2 sec. The vertical scale is relative and arbitrary. Sampling is 50 data points/km.

flown at any desired aircraft speed with subsequent reprocessing of the recorded data reducing the effective survey speed to zero, thus removing spatial distortion. In practice, however, the ultimate sensitivity of geophysical instrumentation will continue to be a factor limiting flight speeds in most airborne surveys.

THEORY

For an aircraft moving with velocity v, a spatial interval Δx along the flight line is recorded as an equivalent temporal interval

$$\Delta t = \Delta x / v.$$

Thus, the recorded time series of geophysical data $g(t)$ represents an equivalent space series $g(vt)$. If the time series is passed through a causal reactive filter having impulse response $h(t)$ before its recording, the time series and, consequently, the equivalent space series are modified according to the convolution

$$g'(t) = \int_{-\infty}^{t} g(\xi)\, h(t-\xi)\, d\xi. \qquad (1)$$

Equivalently, in the angular frequency (ω) domain of the Fourier transformation we have

$$G'(\omega) = G(\omega) \cdot H(\omega), \qquad (2)$$

where $H(\omega)$ is the filter's transfer function, and where

$$G(\omega) = \int_{-\infty}^{\infty} g(t)\, e^{-j\omega t} dt, \qquad (3)$$

and

$$G'(\omega) = \int_{-\infty}^{\infty} g'(t)\, e^{-j\omega t} dt,\ j = \sqrt{-1} \qquad (4)$$

are the Fourier transforms of the data series and filtered data series, respectively.

A single-stage reactive integrator is represented by the transfer function

$$H(\omega) = \frac{1}{1 + j\omega\tau}, \qquad (5)$$

where τ is the time constant of integration usually determined by a resistor(R)-capacitor(C) pair

$$\tau = RC. \qquad (6)$$

While achieving the purpose of reducing components of the data having frequencies $\omega > 1/\tau$ to eliminate spatial noise, we see that the integrator introduces a frequency-dependent phase shift as well,

$$\phi(\omega) = \tan^{-1}(-\omega\tau). \qquad (7)$$

For $\omega\tau \gg 1$, phases are delayed by $\pi/2$ radians, and even at the cut-off or corner frequency of the integrator ($\omega_c = 1/\tau$) phases are delayed by $\pi/4$ radians. Thus, the high-frequency components of the geophysical space series are being effectively delayed by

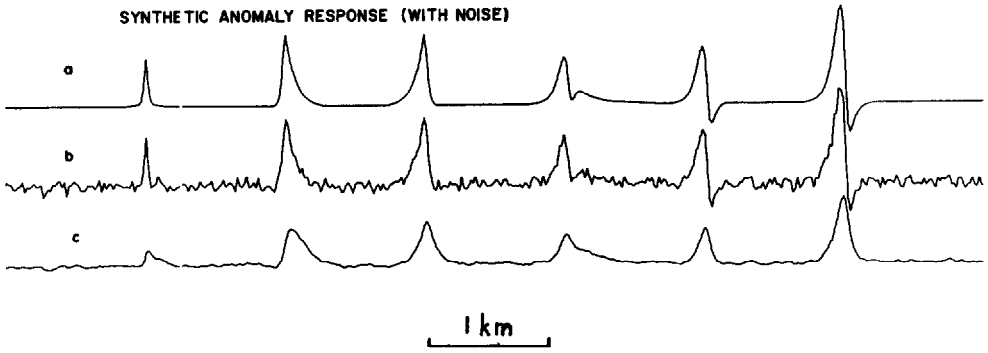

FIG. 2. The reduction of high-frequency noise by in-aircraft low-pass filtering based upon the reactive integrator. To the synthetic anomaly series (a) of Figure 1a white Gaussian noise has been added (b). The low-pass filtering removes the high spatial frequency components of the noise (c).

the filtering process, introducing an often serious distortion.

In Figure 1a we show six synthetic geophysical model anomalies as might be recorded in a survey aircraft traveling at zero velocity. The first and second three anomalies are of the shape that would be obtained with the Scintrex Tridem system and the McPhar F-400 system (Ghosh and West, 1971), respectively. Figure 1b shows the effect of recording these anomalies through an integrator filter with time constant τ of 2 sec in a survey aircraft flying from left-to-right at a standard 40 m/sec. Noticeable distortion is apparent; in the worst cases of sharpest artificial anomalies, the anomaly peaks are delayed ("dragged downstream") by as much as 100 m.

Figure 2 shows the series of anomalies (a) of Figure 1a to which has been added spectrally white Gaussian noise (b) intended to represent, for example, instrument noise, random atmospheric noise, shallow geologic effects, and sensor orientation variations. Figure 2c shows this noisy anomaly series as recorded by the moving aircraft's integration-recording system.

In principle, the aim of the integration has been only to eliminate high-frequency noise from the data to avoid its aliasing upon subsequent analog-to-digital conversion in the recording process or simply to remove the random component of the data which masks useful geophysical anomalies. The attendant distortion or dispersion of the data series is clearly an undesirable side effect. Fortunately, by employing an inverse phase-compensating filter, phases can be readjusted without seriously affecting the amplitudes of the filtered data components.

The nonrealizable, but nonphase-shifting (or zero-phase), filter which has an amplitude response identical to that of the chosen in-aircraft integrator [equation (5)], is described by transfer function

$$H_I(\omega) = \frac{1}{(1 + \omega^2\tau^2)^{1/2}}. \tag{8}$$

Upon direct Fourier transformation of this ideal filter's transfer function [equation (8)], we obtain (Erdélyi, 1954)

$$\begin{aligned} h_I(t) &= \frac{1}{\pi\tau} K_0\left(\frac{t}{\tau}\right), \; t \geq 0, \\ &= \frac{1}{\pi\tau} K_0\left(-\frac{t}{\tau}\right), \; t < 0, \end{aligned} \tag{9}$$

where $K_0(Z)$ is the *zero*th-order modified Hankel function, Z being its generally complex argument. The required phase-compensating filter $H_{PC}(\omega)$ is one which, when applied in series with the in-aircraft integrator (i.e., probably following recording), provides the equivalent ideal overall response $H_I(\omega)$ of equation (8)

$$H_I(\omega) = H(\omega) \cdot H_{PC}(\omega). \tag{10}$$

The transfer function of the appropriate phase-compensating filter is then simply

$$H_{PC}(\omega) = \frac{1 + j\omega\tau}{(1 + \omega^2\tau^2)^{1/2}} = \sqrt{\frac{1 + j\omega\tau}{1 - j\omega\tau}}, \tag{11}$$

and from (Erdélyi, 1954)

$$h_{PC}(t) = \frac{1}{\pi\tau}[K_0(t/\tau) + K_1(t/\tau)], \quad t > 0,$$

$$= \frac{1}{\pi\tau}[K_0(t/\tau)], \quad t = 0,$$

$$= \frac{1}{\pi\tau}[K_0(-t/\tau) - K_1(-t/\tau)], \quad t < 0, \tag{12}$$

where $K_1(Z)$ is the first-order modified Hankel function.

In rough principle, direct application of this filter via multiplication of its transfer function with the Fourier transform $G'(\omega)$ of the recorded data series $g'(t)$ obtains the Fourier transform $G_I(\omega)$ of the desired nondispersed geophysical data,

$$G_I(\omega) = G'(\omega) \cdot H_{PC}(\omega), \tag{13}$$

or equivalently in the time domain by convolution, a phase-compensated data series

$$g_I(t) = \int_{-\infty}^{\infty} g'(\zeta)\, h_{PC}(t - \zeta)\, d\zeta. \tag{14}$$

Of course, it is well known that for real data, this direct approach cannot be executed because one cannot obtain $G'(\omega)$ from a finite data series. Moreover, the filter $h_{PC}(t)$ generally has an infinite-duration, acausal time response so that the effects of the filter's memory of its interaction with the beginning and end of a finite data sample must affect all filtered data. Consequently, we can never hope to obtain precisely the phase-compensated finite series $g_I(t)$ from a finite sample of the infinite data time series $g'(t)$.

However, we can diminish this problem by appropriately approximating $h_{PC}(t)$ with a truncated filter $h_{PCT}(t)$ which is defined as nonzero only over some finite range of $-T < t < T$. Then, if the duration of this truncated filter is sufficiently shorter than the survey data series sample, we shall be able to obtain approximately phase-compensated data.

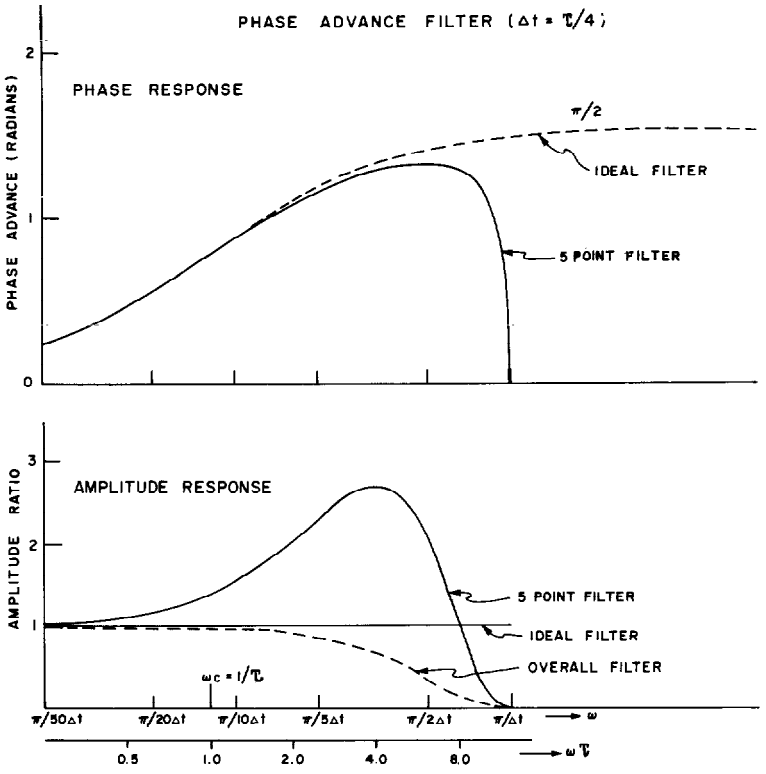

FIG. 3. The phase (above) and amplitude (below) response of the 5-point phase-compensation filter compared to an ideal filter. The combined (overall) amplitude response of the in-aircraft integrator and the 5-point filter in series also is shown. In spite of the enhancement of high-frequency components by the short filter, the combined response provides effective attenuation of high-frequency noise.

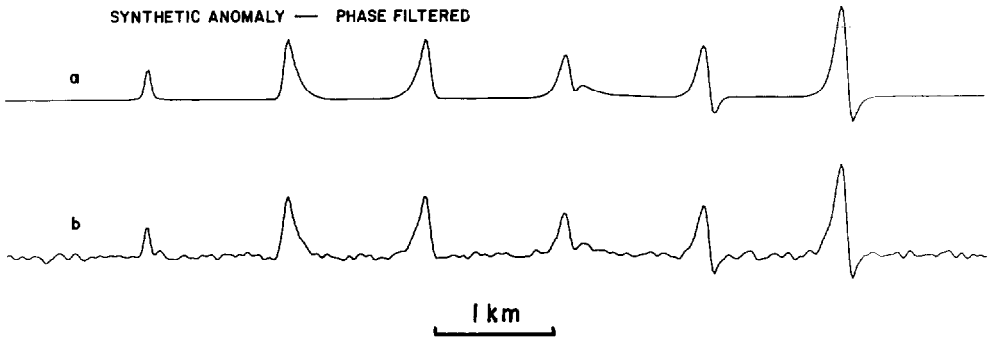

FIG. 4. Phase-compensation of the integrator-distorted synthetic anomaly data series of Figures 1 and 2. (a) For noise-free data, the assymetries produced due to the flight direction across the synthetic anomalies is completely eliminated. The effect of the phase-compensation filter is to reduce the speed of the aircraft to zero. (b) For noisy data, the anomaly shapes are corrected by the short 5-point filter, although some of the high-frequency noise is also amplified. Sampling is 50 data points/km.

The art of digital filter design usually involves obtaining a sufficiently accurate, while economically short, approximation to a desired ideal filter. Several design approaches are valid. For example, one might require filter errors to fall within certain limits, then obtain the shortest filter which can fulfill this criterion. In general, increased accuracy in the frequency reponse of a filter requires a longer filter operator which will shorten the useful length of the filtered data series. For an excellent summary of the principles of digital filter design, see Oppenheim and Schafer (1975, chap. 5).

A direct approach to obtain the required digital filter involves sampling of the design filter's continuous impulse response after it has been zero-phase low-pass filtered. The sampling interval is chosen to be equivalent to the data series interval, while the low-pass filter's cut-off frequency is chosen to be low enough to eliminate possible aliasing of the required digital filter. This digital filter is truncated to the desired length with one of the many standard data windows (e.g., Parzen, Bartlett, Lanczos, etc.). In the case of the phase-compensating filter, the impulse response is quite complicated, involving special functions, and consequently these design procedures must involve careful numerical analysis.

Rather than using the direct approach mentioned above, we shall investigate the performance of the shortest possible phase-compensating filter using the simulated anomaly data series as a test. It will be shown that even this very short filter is capable of useful phase compensation.

To find the shortest phase-compensating filter, we note that $h_{PC}(t)$ of equation (12) can also be written

$$h_{PC}(t) = [\delta(t) + \tau\delta'(t)] * h_I(t), \quad (15)$$

where $\delta(t)$ is the well-known Dirac delta function, and $\delta'(t)$ is its first temporal derivative,

$$\delta'(t) = \lim_{\varepsilon \to 0} \frac{1}{2\varepsilon}[\delta(t+\varepsilon) - \delta(t-\varepsilon)]. \quad (16)$$

As before,

$$h_I(t) = \frac{1}{\pi\tau} K_0\left(\frac{|t|}{\tau}\right). \quad (17)$$

Furthermore, we note that $h_I(t)$ contributes only to attenuation of high-frequency spectral components. The phase is properly compensated entirely by the leading factor of the convolution

$$p(t) = \delta(t) + \tau\delta'(t). \quad (18)$$

Thus, a possible method for obtaining the desired phase-compensating filter is to combine sufficiently accurate approximations to $p(t)$ and $h_I(t)$ in a series configuration. A simple zero-phase low-pass filter is provided by the Bartlett function

$$\begin{aligned} q(t) &= \frac{1}{T}\left(1 - \frac{|t|}{T}\right), & |t| \le T, \\ &= 0, & |t| > T, \end{aligned} \quad (19)$$

which has the well-known transfer function

$$Q(\omega) = \left(\frac{\sin \omega T}{\omega T}\right)^2. \quad (20)$$

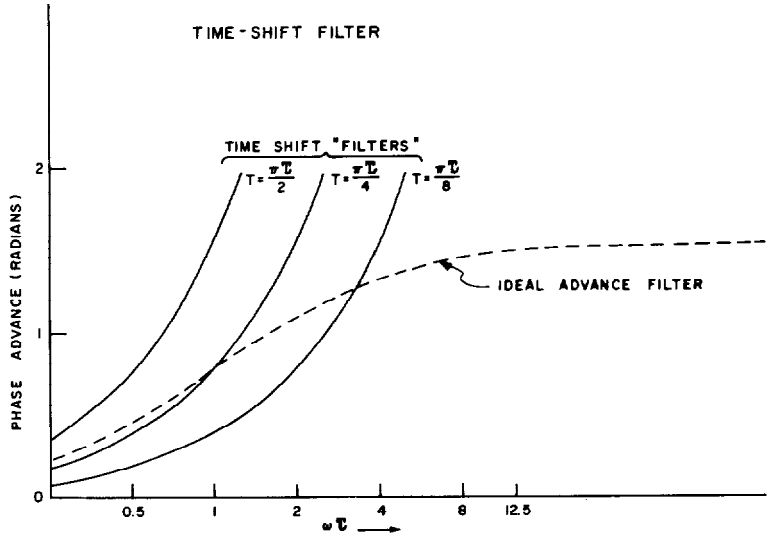

FIG. 5. The phase compensation of the simple time-advance equivalent filter. Note that a time advance of $T = (\pi/4)\tau$ produces the best approximation to the required phase compensation at frequencies below the corner ($\omega\tau = 1$).

A very short digital filter approximation to the ideal phase-compensating filter can be obtained by letting $\varepsilon = \Delta t$, the data sample interval, in the limiting formula for $\delta'(t)$ [equation (16)]

$$p(m) = \begin{cases} \tau/2\Delta t & m = -1 \\ 1 & m = 0 \\ -\tau/2\Delta t & m = +1 \\ 0 & |m| > 1 \end{cases}, \qquad (21)$$

and by approximating the continuous low-pass filte function $h_I(t)$ of equations (9) and (17) by the 3-point Bartlett digital filter

$$q(m) = \begin{cases} \frac{1}{2} & m = 0 \\ \frac{1}{4} & m = \pm 1, \\ 0 & |m| > 1 \end{cases} \qquad (22)$$

where m is the data sample time index. The coefficients which phase compensate for a single stage of integration with time constant τ are then simply

$$h_{PCT}(m) = p(m) * q(m) = \left(\frac{\tau}{8\Delta t}, \frac{1}{4} + \frac{\tau}{4\Delta t}, \frac{1}{2}, \frac{1}{4} - \frac{\tau}{4\Delta t}, -\frac{\tau}{8\Delta t}\right) \qquad (23)$$

The amplitude and phase response for this shortest digital filter with $\tau = 2$ sec and $\Delta t = 0.5$ sec are compared to the ideal continuous filter's response characteristics in Figure 3. Note that phase is very well compensated, remaining within 0.3 degrees, to the cut-off frequency $\omega_c = 1/\tau$, while amplitudes are not seriously affected over the passband of the integrator. The combined response of the in-aircraft reactive integrator in series with this digital phase-compensating filter also is shown. Even three octaves beyond the integrator's cut-off frequency, the overall phase error does not exceed 9 degrees. At these higher frequencies, amplitudes of harmonic components in the data are attenuated 18 dB by the in-aircraft integrator (more than 17 dB overall) and thus contribute very little to the shape of the anomaly. As can be seen in Figure 4a, this shortest filter produces highly satisfactory phase compensation which noticeably reduces the one-sided distortion of the synthetic anomaly forms. Though marginally improved performance could be obtained through the use of much longer numerical filters, such filters are probably not worth the added expense of computation. However, it should be stated that, providing one is willing to pay the costs involved in the use of long filters, arbitrarily precise phase compensation for all frequencies below the sampled data's Nyquist frequency $f = 1/2\Delta t$ is possible through their use. Furthermore, while these short filters tend to enhance frequencies somewhat beyond the integrator's cut-off frequency, thus reintroducing some of the noise components into the data (see Figure 4b), the use of long filters could virtually eliminate this minor problem.

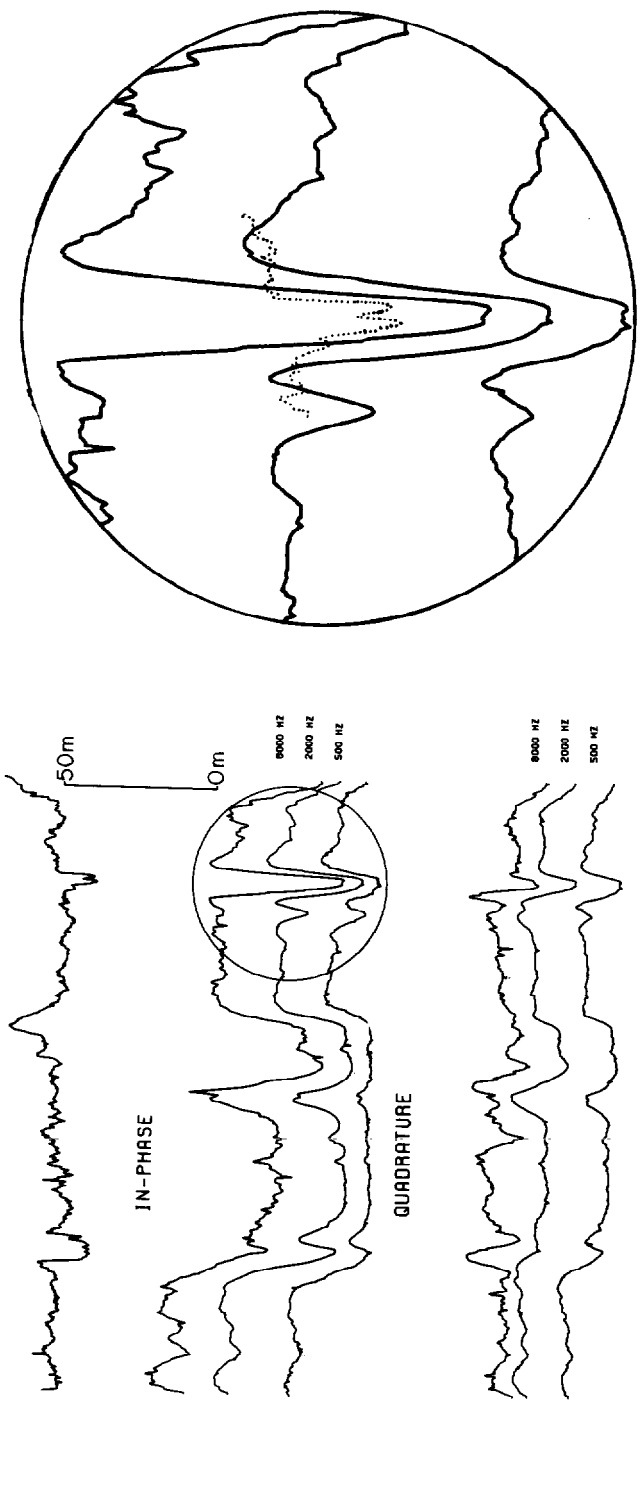

FIG. 6. Data from a Tridem-AEM survey in the Hawksbury, Ontario area showing both the in-phase and quadrature components of the data at three frequencies. Note that the record of altitude above the ground surface in meters is shown above the figure. Circled details: the in-phase anomaly due to the limestone outcrop; the altitude record (dotted) is superimposed. Sampling is 50 data points/km.

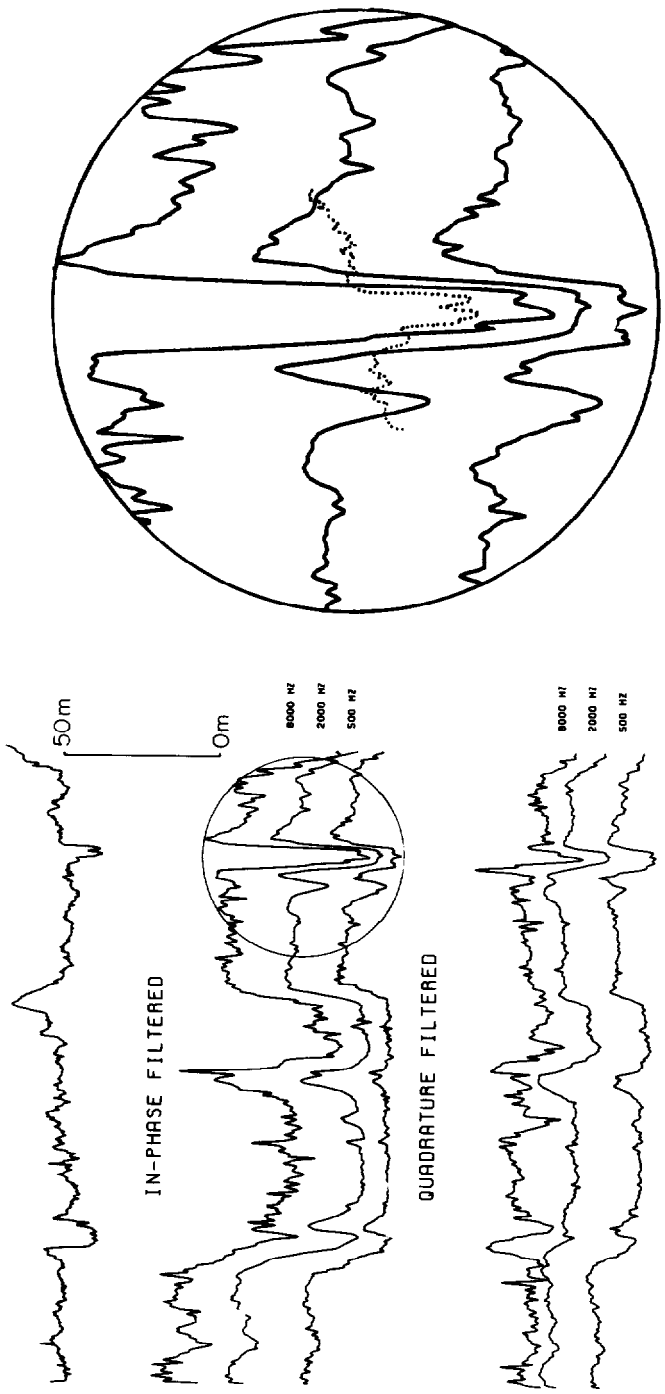

FIG. 7. Phase compensation applied to Hawksbury, Ontario survey data shown in Figure 6. The phase-compensated in-phase and quadrature components of the data at three frequencies are shown. Circled details: phase compensation of the highly resolved anomaly due to the outcrop reduces distortion. The phase-compensating filter design was based on the 2-sec integration constant used in this survey. Sampling is 50 data points/km.

PRACTICAL CONSIDERATIONS

To place this work in its proper context, one should recall that geophysicists have always employed a crude form of phase compensation in aerogeophysical survey interpretation, that is, by means of a simple spaceshifting of the data series to force its alignment with the true geophysical anomaly structure. Clearly, this method does nothing to reduce the distortion of the true anomaly's shape.

A time advance of T sec represents a filter with equivalent impulse response

$$h_T(t) = \delta(t + T), \tag{24}$$

and transfer function

$$H_T(\delta) = e^{j\omega T}. \tag{25}$$

One sees that this filter possesses the desired unit gain and accomplishes a linear phase advance

$$\phi(\omega) = \omega T. \tag{26}$$

By appropriately choosing T, one can approximate ideal phase compensation over some small range of frequencies. For example, in the usual application, T is chosen equal to $(\pi/4)\tau$ so that at $\omega_c = 1/\tau$ the phase is properly advanced by $\pi/4$. However, substantial phase errors exist at frequencies not sufficiently close to ω_c. Figure 5 shows a comparison of the ideal phase compensation with the phase compensation obtained using three particular time advances. A time advance of $(\pi/4)\tau$ does provide for reasonably accurate phase compensation at frequencies below the integrator's cut-off at $\omega = 1/\tau$. While this linear phase-advance filter does best align the data, its incomplete phase compensation is seen in the continuing distortion of the anomaly shape.

In many cases, however, this *zero*th approximation to phase compensation can produce a useful result. Providing the true anomaly possesses high spatial frequency components with only very low amplitudes and Giret's (1962) criterion is sufficiently well met, this simple data realignment should be adequate. But if, for economy, we choose to violate Giret's rule-of-thumb, significantly increasing the aircraft speed-integration time constant product beyond the flight elevation, we quickly reach a point where the amount of anomaly distortion becomes unacceptable. We then are required to apply a better approximation to the ideal phase compensation. For any reasonable survey situation, the 5-point filter described above will probably be adequate.

THE HAWKSBURY SURVEY

In 1972, the Geological Survey of Canada sponsored a survey of approximately 200 line-km over an area near Hawksbury, Ontario to demonstrate the Tridem AEM system. A nominal flight altitude of 50 m was used, the flight speed being 40 m/sec. To eliminate aliasing of high frequencies upon digital recording of the data with a sampling interval of $\Delta t = 0.5$ sec and to reduce atmospheric and orientation noise, the three signals (carrier frequencies at 500 Hz, 2000 Hz, and 8000 Hz, respectively) were integrated in-aircraft with a time constant of $\tau = 2$ sec (Figure 6). The aircraft speed-time constant product somewhat exceeds the flight altitude, which, according to Giret's criterion, suggests that highly resolved anomalies could be distorted in shape. Using both the in-phase and quadrature data obtained during one 16-km flight line, phase-compensating filtering was applied using the appropriate 5-point short filter

$$h_{PCT}(m) = (0.5,\ 1.25,\ 0.50,\ -0.75,\ -0.50). \tag{27}$$

As the low-frequency (500 Hz) data provide so little anomaly resolution, the benefits of the phase compensation (compare Figures 6 and 7) are not evident. Rather, the filter has only accomplished the trivial result of properly realigning the space-series data with the true geophysical anomaly, time-advancing the data by about 1.6 sec, and equivalently space-advancing it by 63 m. The mid-frequency (2000 Hz) record shows only a marginal reduction of the distortion of anomaly shapes. However, the high-frequency (8000 Hz) record, which has the highest resolution, is usefully phase-corrected, as can be determined by careful comparison of the filtered and unfiltered records in the circled details shown in Figures 6 and 7. As well as properly realigning the data with the true anomaly structure, the most highly resolved features of the anomalies are noticeably changed in shape.

In particular, there is an outcrop of highly resistive limestone, the area being generally covered by a conductive clay. This outcrop is visible in the dotted altitude record superimposed on the data shown in the circled details of Figures 6 and 7. On this altitude record, we measure the outcrop relief to be approximately 10 m over a width of about 275 m. Also, a hump is seen at each edge of the outcrop having a further elevation of 1 to 2 m and an apparent width of approximately 40 m. One would expect such a structure to produce an anomaly with a magnitude roughly inversely related to the separation between the aircraft

and the outcrop. Thus, one would obviously suggest that the greater anomaly magnitude should be seen corresponding to the leading edge of the structure where its elevation is greatest, bringing it closest to the aircraft. The effect of the integrator-produced phase distortion of the data produces just the opposite result: the anomaly maximum is phase-delayed, apparently occurring coincident with the trailing edge of the outcrop structure (Figure 6). The phase compensation (Figure 7) removes this distortion, properly placing the anomaly maximum at the outcrop's leading edge, approximately 150 m earlier along the flight line.

CONCLUSION

The example above demonstrates the conditions under which phase compensation is useful: (1) high spatial frequency content in anomaly shape, (2) a survey resolution capability to achieve scales less than the integrator time constant-aircraft velocity product, and (3) high-quality, high-sensitivity data.

Given sufficient survey resolution, even a higher degree of relief variability across the outcrop would have produced a result similar to that seen above. In a reversed situation where, for example, a highly conducting body is buried in a low-conductivity host rock, a high-resolution AEM survey could shift a sharp anomaly maximum more than 100 m down the flight line due purely to phase distortion. A best target for surface detailing and drilling conceivably could be missed.

Finally, aerogeophysical surveys are often flown in alternating directions on adjacent flight lines. Due to in-aircraft reactive filtering, the high spatial frequency components of anomalies are always moved some distance along the flight line, causing distortion of anomaly details. In correcting for alignment but not for distortions, automatic contouring procedures can produce the well-known "herringbone effect" often seen in high-resolution aerogeophysical maps. Although for many types of surveys there are other contributions to this effect, it is easily possible to remove that contribution which is caused simply by the in-aircraft reactive filtering. Since substantial costs are incurred in any form of digital data processing, such as production of contour maps, it would seem very worthwhile to remove phase distortion, as the additional cost certainly is insignificant.

ACKNOWLEDGMENTS

This research was supported by research grants from the National Research Council of Canada to O. G. Jensen and A. Becker. The authors wish to thank the Geological Survey of Canada for providing the data from the Hawksbury, Ontario area. The efforts of J. Roy and Scintrex Ltd. are gratefully acknowledged.

REFERENCES

Erdélyi, A., 1954, Tables of integral transforms, v. 1: New York, McGraw-Hill Book Co., Inc.

Ghosh, M. K., 1972, Intepretation of airborne EM measurements based on thin sheet models: Unpubl. Ph.D. thesis, Univ. of Toronto.

Ghosh, M. K., and West, G. F., 1971, AEM analog model studies: Toronto, Paterson & Associates Ltd.

Giret, M. R., 1962, Effet de la vitesse et de la constante d'integration sur la forme des anomalies aeroradiometriques: Geophys. Prosp., v. 10, p. 183–202.

Oppenheim, A. V., and Schafer, R. W., 1975, Digital signal processing: Englewood Cliffs, NJ, Prentice-Hall.

Palacky, G. J., 1976, Use of decay patterns for the classification of anomalies in time-domain AEM measurements: Geophysics, v. 41, p. 1031–1041.